Cancer Cell
Article

Tumor Suppression by Phospholipase C-β3 via SHP-1-Mediated Dephosphorylation of Stat5

Wenbin Xiao,[1] Hong Hong,[1] Yuko Kawakami,[1] Yuko Kato,[2] Dianqing Wu,[3,4] Hiroki Yasudo,[1] Akiko Kimura,[5] Hiromi Kubagawa,[6] Luigi F. Bertoli,[8] Randall S. Davis,[7] Luan A. Chau,[9] Joaquin Madrenas,[9] Cyrus C. Hsia,[10] Anargyros Xenocostas,[10] Thomas J. Kipps,[11] Lothar Hennighausen,[5] Atsushi Iwama,[2] Hiromitsu Nakauchi,[12] and Toshiaki Kawakami[1,*]

[1]Division of Cell Biology, La Jolla Institute for Allergy and Immunology, La Jolla, CA 92037, USA
[2]Department of Cellular and Molecular Medicine, Graduate School of Medicine, Chiba University, Chiba 260-8670, Japan
[3]Program for Vascular Biology and Therapeutics
[4]Department of Pharmacology
Yale University School of Medicine, New Haven, CT 06520, USA
[5]Laboratory of Genetics and Physiology, National Institutes of Health/National Institute of Diabetes and Digestive and Kidney Diseases, Bethesda, MD 20892, USA
[6]Department of Pathology
[7]Department of Medicine
University of Alabama, Birmingham, AL 35294, USA
[8]Brookwood Medical Center, Birmingham, AL 35209, USA
[9]Department of Microbiology and Immunology, University of Western Ontario, London, ON N6A 5K8, Canada
[10]Department of Medicine, University of Western Ontario, London, ON N6A4G5, Canada
[11]Department of Internal Medicine, University of California, San Diego, La Jolla, CA 92093, USA
[12]Laboratory of Stem Cell Therapy, Center of Experimental Medicine, Institute of Medical Science, University of Tokyo, Tokyo 108-8639, Japan
*Correspondence: toshi@liai.org
DOI 10.1016/j.ccr.2009.05.018

SUMMARY

Given its catalytic activity to generate diacylglycerol and inositol 1,4,5-trisphosphate, phospholipase C (PLC) is implicated in promoting cell growth. However, we found that PLC-β3-deficient mice develop myeloproliferative disease, lymphoma, and other tumors. The mutant mice have increased numbers of hematopoietic stem cells with increased proliferative, survival, and myeloid-differentiative abilities. These properties are dependent on Stat5 and can be antagonized by the protein phosphatase SHP-1. Stat5-dependent cooperative transformation by active c-Myc and PLC-β3 deficiency was suggested in mouse lymphomas in *PLC-β3*$^{-/-}$ and in *Eμ-myc;PLC-β3*$^{+/-}$ mice and human Burkitt's lymphoma cells. The same mechanism for malignant transformation seems to be operative in other human lymphoid and myeloid malignancies. Thus, PLC-β3 is likely a tumor suppressor.

INTRODUCTION

The production and lineage commitment of hematopoietic cells is controlled by the actions of a multitude of cytokines, growth factors, and hormones (Kondo et al., 2003). Cell surface receptors bound by these ligands activate several signaling pathways including the Jak-Stat pathway. This pathway plays a crucial role in a number of biological functions by activating transcription of various target genes (Levy and Darnell, 2002; O'Shea et al., 2002; Schindler et al., 2007). Cytokine stimulation activates Jak kinases through transphosphorylation and results in tyrosine phosphorylation of receptor sites, Stats, and other substrates.

SIGNIFICANCE

Many hematopoietic malignancies depend on the activity of Stat5 transcription factor. Here, we report a novel Stat5-suppressive mechanism by which PLC-β3 augments dephosphorylating activity of SHP-1 toward Stat5 by recruiting SHP-1 and Stat5 to its C-terminal sequence. Abrogation of this suppression leads to myeloproliferative disease, lymphoma, and other types of cancer in *PLC-β3*$^{-/-}$ mice. PLC-β3 deficiency or downregulation appears to cooperate with c-Myc to induce B cell lymphoma in mice and humans. The same mechanism may be operative in human myeloid and lymphoid tumors. Therefore, the adaptor function of PLC-β3 seems essential to protect the hematopoietic and nonhematopoietic systems from tumor development.

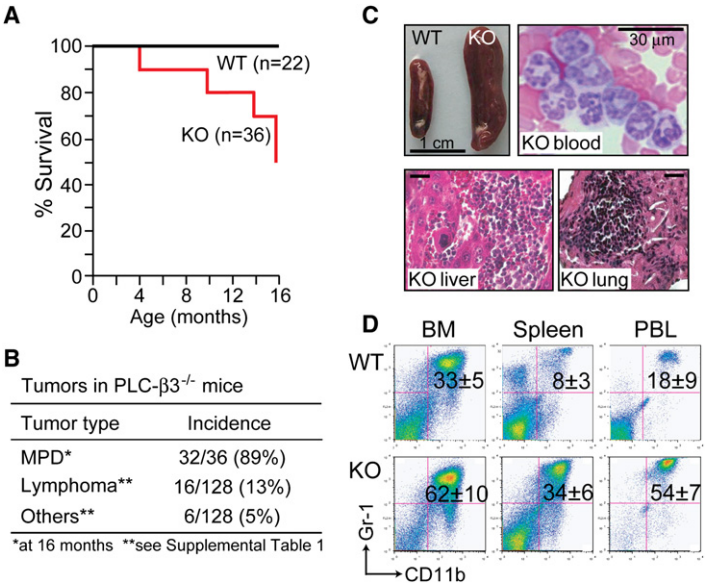

B

Tumors in PLC-β3$^{-/-}$ mice

Tumor type	Incidence
MPD*	32/36 (89%)
Lymphoma**	16/128 (13%)
Others**	6/128 (5%)

*at 16 months **see Supplemental Table 1

Figure 1. *PLC-β3*$^{-/-}$ Mice Develop MPD, Lymphoma, and Other Tumors

(A) Survival analysis.

(B) Summary of tumors developed in *PLC-β3*$^{-/-}$ mice.

(C) Hematologic analysis of 10-month-old *PLC-β3*$^{-/-}$ mice. Splenomegaly in *PLC-β3*$^{-/-}$ mice (top left) was associated with effaced splenic architecture (data not shown). Increased mature granulocytes in *PLC-β3*$^{-/-}$ mice were shown by blood smear (top right) and hematoxylin and eosin staining of lung and liver sections (bottom). Bars in tissue sections indicate 30 μm.

(D) Flow cytometric analysis of nucleated cells in BM, spleen, and peripheral blood leukocytes (PBL) from 10-month-old mice (n = 16). Granulocytes (CD11b$^+$/Gr-1$^+$; percentages ± SD shown) were increased in these organs of aged *PLC-β3*$^{-/-}$ mice.

Following tyrosine phosphorylation, Stats homo- or heterodimerize, translocate to the nucleus, and activate gene expression through sequence-specific response elements.

To date, seven mammalian Stat family members have been identified: Stats 1, 2, 3, 4, 5A, 5B, and 6; Stat5 is encoded by two recently duplicated genes, *Stat5A* and *Stat5B*, with ~96% sequence identity (Mui et al., 1995). Stat5 plays a crucial role in early hematopoiesis—*Stat5A* and *Stat5B* doubly disrupted mice displayed a profound defect in competitive repopulation of hematopoiesis (Bunting et al., 2002; Snow et al., 2002). The commitment of embryonic stem cells to hematopoietic cells is augmented by a Stat5-mediated signal (Kyba et al., 2003). Stat5 also plays a role in myeloid cell proliferation and differentiation (Ilaria et al., 1999). Constitutive activation of Stat5 in human cord blood CD34$^+$ cells enhances their capacity to repopulate NOD/SCID mice and promotes erythroid differentiation (Schuringa et al., 2004). Constitutively active Stat5 promotes self-renewal, proliferation, and survival of mouse hematopoietic stem cells (HSC) and induces a lethal myeloproliferative disease (MPD) in mice (Kato et al., 2005).

Stat signals are downregulated by three well-characterized mechanisms: dephosphorylation, nuclear export, and suppressor of cytokine signaling (SOCS) feedback inhibition (Shuai, 2000; Tanaka et al., 2005). SOCS proteins bind either activated Jak proteins or cytokine receptors to inhibit Jak activity (Alexander and Hilton, 2004). Several protein tyrosine phosphatases have been reported to dephosphorylate either Jak and/or Stat proteins. For example, Jak2 interacts with SHP-1 and may be dephosphorylated by SHP-1 (Jiao et al., 1996; Klingmuller et al., 1995).

Phospholipase C-β (PLC-β) is a small family of enzymes that can produce diacylglycerol and IP_3 downstream of heterotrimeric G proteins (Rhee, 2001). As diacylglycerol can activate protein kinase C (PKC), and IP_3 can mobilize Ca^{2+}, PLC-β is implicated in promoting cell proliferation. PLC-β directly interacts with GTP-bound Gα subunits, leading to its catalytic activation. The four isoforms of PLC-β (β1–β4) show different tissue expression specificity and heterotrimeric G protein regulation profiles. PLC-β1 and PLC-β3 are expressed in a wide range of tissues and cell types, while PLC-β2 and PLC-β4 are expressed only in hematopoietic and neuronal tissues, respectively. PLC-β2 and PLC-β3 can also be activated by βγ subunits of the $G\alpha_{i/o}$ family of G proteins (Camps et al., 1992; Katz et al., 1992; Lee et al., 1993). Consistent with their roles in G protein-coupled receptor signaling, chemokine-induced IP_3 production, Ca^{2+} signaling, and migration are reduced in *PLC-β2*$^{-/-}$ and *PLC-β2*$^{-/-}$*;PLC-β3*$^{-/-}$ neutrophils (Li et al., 2000) and T cells (Bach et al., 2007). However, little is known about the role of these PLC-β isoforms in hematopoiesis or tumorigenesis. Here we have studied the role of PLC-β3 in these processes using *PLC-β3*$^{-/-}$ mice.

RESULTS

PLC-β3-Deficient Mice Develop Various Tumors Including MPD and Lymphoma

PLC-β3 deficiency led to a premature death in mice (Figure 1A). Fifty percent (18 of 36 mice) of *PLC-β3*$^{-/-}$ mice died within an observation period of 16 months, in contrast with 100% survival of wild-type (WT) mice. By the age of 16 months, most *PLC-β3*$^{-/-}$ mice in this cohort exhibited splenomegaly (Figure 1B-C), the incidence of which reached 89% when prematurely dead mice with this abnormality were included. The enlarged spleens had effaced architecture characterized by markedly increased myeloid cells and some erythroid cells, indicative of extramedullary hematopoiesis (data not shown). Livers and lungs also had foci composed of myeloid cells (Figure 1C). Dramatic increases in CD11b$^+$Gr-1$^+$ mature granulocytes in bone marrow (BM), spleen, and peripheral blood from these mice were observed (Figures 1C and 1D and see Tables S1 and S2 available with this article online). Microbiological examinations showed no indications of bacterial infection in the diseased mice, and antibiotic treatments did not affect the number of granulocytes (data not shown). Therefore, these hematologic findings were consistent with the diagnosis of MPD (Kogan et al., 2002), unlike myelodysplastic syndrome that is frequently associated with anemia.

During a 2 year observation period, three in another cohort of 16 *PLC-β3*$^{-/-}$ mice with increased granulocytes developed anemia (hematocrits of 11%, 16%, and 22%) with increased numbers of blast cells in their BM (32%, 35%, and 45%, respectively). This result suggests that the MPD can evolve to accelerated and blast-crisis stages, similar to human chronic myelogenous leukemia (CML) (Sawyers, 1999). Gross and histologic

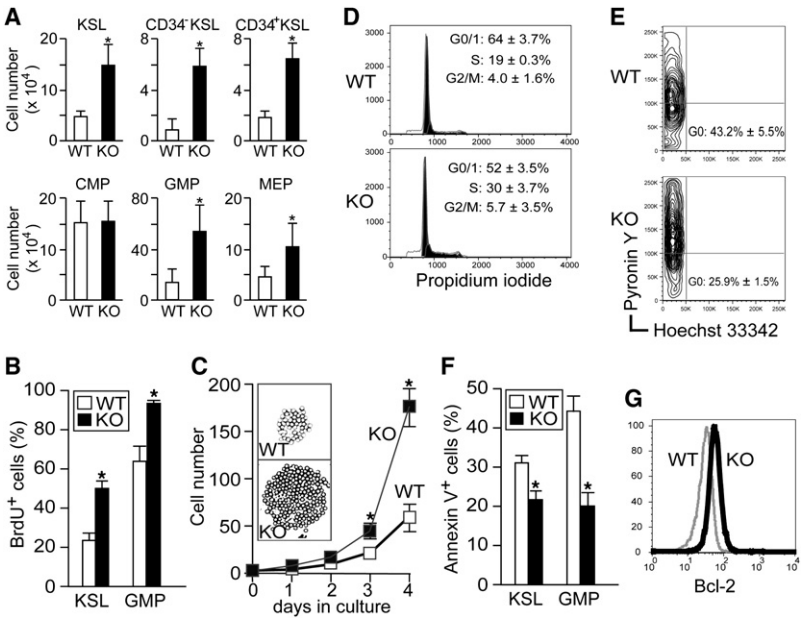

Figure 2. Increases in KSL Cells and GMP in *PLC-β3*$^{-/-}$ Mice Are Due to Increased Proliferation and Decreased Apoptosis

(A) BM cells from 10-month-old mice (n = 16) were subjected to flow cytometric analysis of HSC and myeloid progenitors (see Figure S2 as well). Results shown are representative of at least four measurements.

(B) In vivo BrdU incorporation into KSL and GMP cells in 10-month-old mice (n = 4).

(C) CD34$^-$ KSL cells from 10-month-old mice (n = 4) were sorted into 96-well plates containing IL-3, SCF, IL-11, Flt3L, and TPO, and cultured for 4 days. The inset shows representative colonies generated at the bottom of well on day 4. Representative of four independent experiments.

(D and E) Cell cycle analysis of propidium iodide-stained Lin$^-$ cells (D) and Hoechst 33342 and Pyronin Y-stained (E) KSL cells from 10-month-old mice (n = 4).

(F) Flow cytometric analysis of annexin V$^+$ apoptotic cells in KSL and GMP cells from 10-month-old mice (n = 4). Results in (A)–(F) represent mean ± SD. *p < 0.05 versus WT cells by Student's t test.

(G) Flow cytometric analysis for Bcl-2 expression in Lin$^-$ cells from 10-month-old mice (n = 2).

examinations of a larger number (128 in total) of *PLC-β3*$^{-/-}$ mice revealed various tumors including lymphoma mostly with T cell markers and carcinomas of skin and lung (Figures 1A and 1B and Figure S1 and Table S3). Unlike *PLC-β3*$^{-/-}$ mice, *PLC-β2*$^{-/-}$ mice did not develop tumors or die prematurely (data not shown).

PLC-β3-Deficient Mice Exhibit Increased Numbers of HSC and Myeloid Progenitors as well as Preferential Granulocytic Differentiation

Aged *PLC-β3*$^{-/-}$ mice with splenomegaly had increased numbers of c-Kit$^+$Sca-1$^+$Lineage$^-$ cells (KSL cells; enriched for HSC), granulocyte-macrophage progenitors (GMP), and megakaryocyte-erythroid progenitors in both BM (Figure 2A and Figure S2) and spleen (data not shown), compared to age-matched WT mice. With regards to HSC subpopulations, *PLC-β3*$^{-/-}$ mice had 5-fold more CD34$^-$ KSL (enriched for long-term repopulating HSC) and 3-fold more CD34$^+$ KSL (enriched for short-term repopulating HSC) cells (Figure 2A). Consistent with the immunophenotypic data, *PLC-β3*$^{-/-}$ BM cells and splenocytes gave rise to greater numbers of myeloid colonies than WT cells in methylcellulose medium (Figure S3A and data not shown). Purified *PLC-β3*$^{-/-}$ KSL and myeloid progenitors (CMP and GMP) generated several-fold more granulocyte (CFU-G) colonies of larger sizes than WT cells (Figures S3B–S3D), suggesting that *PLC-β3*$^{-/-}$ HSC and myeloid progenitors have an increased predisposition to differentiate into granulocytes, which is consistent with the MPD phenotype in *PLC-β3*$^{-/-}$ mice. Moreover, *PLC-β3*$^{-/-}$ BM and KSL cells were hypersensitive to cytokines (Figure S3E), a hallmark of human MPDs (Emanuel et al., 1991), and formed macrophage (CFU-M) and granulocyte-macrophage (CFU-GM) colonies in the absence of growth factors (Figure S3F), a feature characteristic of transformed cells.

HSC-Enriched Populations Derived from *PLC-β3*$^{-/-}$ Mice Exhibit Increased Proliferation and Survival

Given the above colony-formation data, blockade of differentiation was ruled out as a contributing factor to the increase in HSC-enriched populations in *PLC-β3*$^{-/-}$ mice. Thus the increase in HSC-enriched populations could be accounted for by increased proliferation, reduced cell death, altered migration, or a combination of these factors. To dissect this point, we first performed in vivo BrdU incorporation experiments in 10-month-old mice. BrdU incorporation into KSL cells was greater in *PLC-β3*$^{-/-}$ mice (Figure 2B and Figure S4A), suggesting increased proliferation in *PLC-β3*$^{-/-}$ HSC-enriched populations. Consistent with this result, *PLC-β3*$^{-/-}$ CD34$^-$ KSL cells grew faster and formed larger colonies than WT cells in the presence of IL-3 or a cytokine cocktail (Figure 2C and data not shown). Cell cycle analysis showed increased proportions of *PLC-β3*$^{-/-}$ lineage$^-$ cells in the S phase and reduced proportions of *PLC-β3*$^{-/-}$ KSL cells in the G_0 phase (Figures 2D–2E). Consistent with the increased proliferation, mRNA levels of the cell cycle inhibitor p19 were reduced, but those of cyclins A2 and B2 increased, in *PLC-β3*$^{-/-}$ KSL cells (Figure S5). We then measured apoptotic cell death in KSL cells by annexin V staining. Apoptosis was less abundant in *PLC-β3*$^{-/-}$ KSL cells (Figure 2F). In line with this, expression of the antiapoptotic protein Bcl-2 was increased in *PLC-β3*$^{-/-}$ KSL cells (Figure 2G). Finally, homing capacity of *PLC-β3*$^{-/-}$ KSL cells was not altered (Figure S6). Therefore, we conclude that the increase in HSC-enriched populations in *PLC-β3*$^{-/-}$ mice is due mainly to increased proliferation and decreased apoptosis. The same mechanisms seem operative in *PLC-β3*$^{-/-}$ GMP (Figures 2B and 2F and Figures S4B and S6B).

The MPD Is Transplantable with HSC-Enriched Populations Derived from *PLC-β3*$^{-/-}$ Mice

The MPD in *PLC-β3*$^{-/-}$ mice was BM cell autonomous, as the irradiated Ly5.1 mice that had received *PLC-β3*$^{-/-}$ BM cells developed MPD within 6–9 months (Table S4). The increased proliferation and survival of *PLC-β3*$^{-/-}$ KSL cells suggested that HSC contain leukemic stem cells (Reya et al., 2001) that cause MPD in *PLC-β3*$^{-/-}$ mice. To test this hypothesis, purified CD34$^-$ KSL, CD34$^+$ KSL, CMP, and GMP from *PLC-β3*$^{-/-}$ and WT mice were transferred into sublethally irradiated

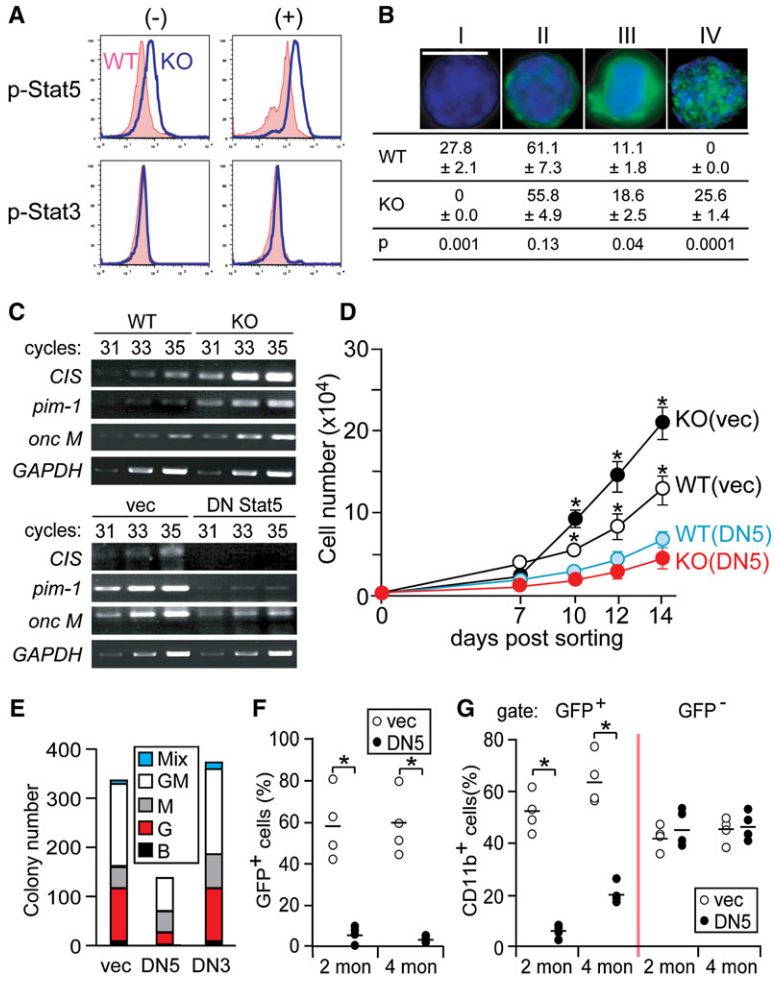

Figure 3. Stat5 Activation Is Required for the Increased Proliferation and Myeloid Differentiation of *PLC-β3*$^{-/-}$ KSL Cells

(A and B) Phospho-Stat5 levels were constitutively (–) higher in *PLC-β3*$^{-/-}$ KSL cells and further increased upon stimulation for 5 min with a cytokine cocktail of IL-3, SCF, IL-11, Flt3L, and TPO (+), as shown by flow cytometric analysis (A) and confocal microscopy (B) with anti-p-Stat5 (Tyr694). Nuclei were stained with DAPI (blue). A bar indicates 10 μm. The patterns of phospho-Stat5 staining in confocal microscopy were categorized into four (I–IV) and their distributions in cytokines-stimulated KSL cells (200 cells counted) from 8- to 10-month-old mice (n = 8) are shown. Representative of four (A) and two (B) independent experiments.

(C) RT-PCR analysis of mRNA expression of Stat5 target genes, *CIS*, *pim*-1, and *oncostain M* in KSL cells from 10-month-old mice (n = 4). Numbers of PCR cycles performed are indicated. GAPDH mRNA is a housekeeping gene control.

(D) CD34^{-} KSL cells were transduced with a bicistronic retroviral vector encoding DN Stat5 (DN5) or DN Stat3 (DN3). GFP^{+} transduced cells were cultured in the presence of IL-3, SCF, IL-11, Flt3L, and TPO. Representative of three independent experiments. Results in (B) and (D) represent mean ± SD.

(E) Transduced cells were cultured in methylcellulose medium containing SCF, IL-3, IL-6, and EPO. B, G, M, GM, and Mix represent BFU-E, CFU-G, CFU-M, CFU-GM, and CFU-Mix, respectively.

(F and G) *PLC-β3*$^{-/-}$ CD34^{-} KSL cells transduced with DN Stat5 or empty vector were adoptively transferred to lethally irradiated C57BL/6-Ly5.1 mice. Two and four months later, peripheral blood was analyzed by flow cytometry for enumeration of GFP^{+} cells (F) and donor-derived CD11b^{+} cells (G). See Table S5 as well. *p < 0.05 by Student's t test.

Rag2$^{-/-}$-Ly5.1 mice. Only *PLC-β3*$^{-/-}$ CD34^{-} KSL cells, but not other cell populations, gave rise to myeloid hyperplasia in recipient mice within only 2 months (Table S4). These results suggest that the leukemic stem cells responsible for the development of MPD in *PLC-β3*$^{-/-}$ mice are present in CD34^{-} KSL cells.

Increased Stat5 Activity Is Critical for Increased Proliferative, Myeloid-Differentiative, and MPD-Causing Capabilities of *PLC-β3*$^{-/-}$ KSL Cells

We next analyzed the signaling pathways accountable for the increased proliferation, survival, and myeloid differentiation of *PLC-β3*$^{-/-}$ KSL cells. Unlike BCR-ABL-induced CML (Sawyers et al., 1995; Skorski et al., 1997), activities of Ras, ERK, and Akt were comparable in WT and *PLC-β3*$^{-/-}$ KSL and mouse embryonic fibroblasts (MEFs) (Figure S7A and data not shown). Importantly, however, Stat5 Tyr-694 phosphorylation was constitutively increased and further induced after stimulation with IL-3 or a cytokine cocktail in *PLC-β3*$^{-/-}$ KSL cells (Figure 3A and Figure S7B) and, compared to WT cells, more frequent and extensive nuclear localization of phospho-Stat5 was observed in *PLC-β3*$^{-/-}$ KSL cells (Figure 3B). In contrast, Stat3 phosphorylation was comparable in *PLC-β3*$^{-/-}$ and WT cells (Figure 3A and Figure S7B). Lymphomas and a skin carcinoma from *PLC-β3*$^{-/-}$ mice also exhibited increased phosphorylation of Stat5, but not Stat3 (Figure 6C and Figure S7C and data not shown). Consistent with Stat5 activation, mRNA expression of Stat5 target genes, e.g., *CIS* (Matsumoto et al., 1997), *pim-1* (Lilly and Kraft, 1997; Nosaka et al., 1999), and *oncostatin M* (Yoshimura et al., 1996), was increased in *PLC-β3*$^{-/-}$ cells (Figure 3C).

To directly test the functional relevance of increased Stat5 activation, we introduced dominant-negative (DN) Stat5 into KSL cells, using a bicistronic retrovirus encoding DN Stat5 and green fluorescent protein (GFP). DN Stat5 induced a reduction in mRNA expression of *CIS*, *pim*-1, and *oncostatin M* (Figure 3C) as expected. DN Stat5 suppressed in vitro expansion of GFP-expressing *PLC-β3*$^{-/-}$ KSL cells (designated as KO/DNStat5 cells) (Figure 3D), suggesting that the increased proliferation/survival depends on the increased Stat5 activity in *PLC-β3*$^{-/-}$ HSC-enriched cells. Colony-forming assays on KO/DNStat5 cells showed a drastic reduction of granulocyte (CFU-G and CFU-GM) colonies compared to KO/vec cells harboring an empty vector (Figure 3E). By contrast, DN Stat3 had little effect on the proliferation and colony-forming abilities of *PLC-β3*$^{-/-}$ and WT cells. Furthermore, the lethally irradiated Ly5.1^{+} mice that had received KO/DNStat5 cells had drastically fewer donor (GFP^{+})-derived blood cells (Figure 3F) and KSL cells (Table S5) than the mice that had received KO/vec cells, indicating that Stat5 is required for engraftment or cell proliferation/survival of the

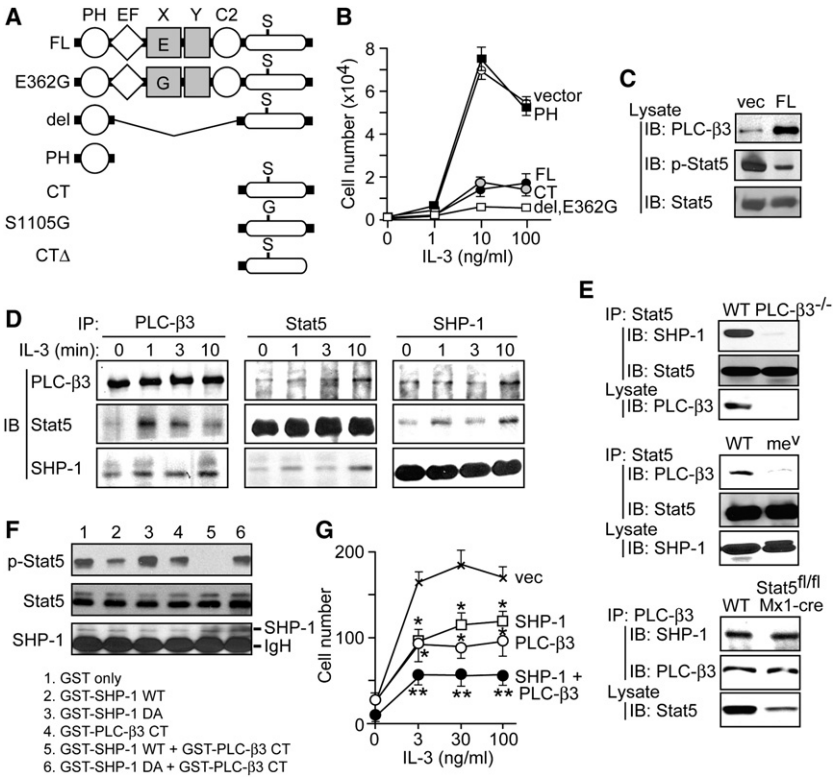

Figure 4. Functional Multimolecular SPS Complexes Contain PLC-β3, Stat5, and SHP-1

(A) Scheme for a panel of PLC-β3 retroviral constructs.

(B) Growth-suppressive function of various PLC-β3 constructs. Ba/F3 cells were transduced with a bicistronic retroviral vector expressing GFP alone (vector) or GFP and either full-length (FL) PLC-β3 or its fragment. Growth responses to the indicated concentrations of IL-3 are shown. S1105G and CTΔ showed almost the same inhibitory effects as CT (data not shown). Similar results were obtained in multiples experiments (at least five times using FL and CT constructs).

(C) FL- and vector-transduced Ba/F3 cells were lysed and directly analyzed by immunoblotting.

(D) Lysates of IL-3-stimulated nontransduced Ba/F3 cells were immunoprecipitated (IP) and followed by immunoblotting (IB) with the indicated antibodies.

(E) Splenocytes from *PLC-β3*$^{-/-}$, *me*^{v}/*me*^{v}, polyI:C-treated *Stat5*$^{fl/fl}$;*Mx1-cre*, and control (WT) mice were analyzed by immunoprecipitation and immunoblotting.

(F) PLC-β3 CT facilitated SHP-1-mediated dephosphorylation of phospho-Stat5 in vitro.

(G) PLC-β3 and SHP-1 synergistically inhibited IL-3-dependent growth of Ba/F3 cells. *$p < 0.05$ and **$p < 0.01$ versus vector control by Student's t test. Results in (B) and (G) represent mean ± SD.

transferred cells as shown by Bunting et al. (2002). Among the GFP^{+} donor cells, the former mice had much fewer CD11b^{+} cells than the latter mice, whereas GFP^{-} cells in mice that had received KO/vec or KO/DNStat5 cells showed high proportions of CD11b^{+} cells similar to those among GFP^{+} cells in mice that had received KO/vec cells (Figure 3G). These results support the notion that the increased Stat5 activity is responsible for the myeloid-differentiative activities of *PLC-β3*$^{-/-}$ HSC-enriched populations. There were increases in myeloid cell percentage from 2 to 4 months after transfer in mice that received both control (vec) and DN Stat5-tranduced cells, suggesting a beginning of MPD development despite the DN Stat5 expression or retroviral inactivation or escape mechanism.

PLC-β3 Suppresses the Growth of Hematopoietic Cells through Its C-Terminal Fragment

IL-3-dependent mouse Ba/F3 cells have been extensively used to investigate Stat5-related signaling events (Warmuth et al., 2007). Expression of PLC-β3 at 2- to 5-fold higher levels over the endogenous level inhibited IL-3-dependent proliferation of Ba/F3 cells, accompanied by reduced Stat5 phosphorylation (Figures 4B and 4C). Next we determined the structural requirements for growth suppression. Importantly, the C-terminal fragment (CT) corresponding to residues 809–1234 retained as strong a growth-suppressive activity as full-length PLC-β3 (Figure 4B). However, the catalytic domain of PLC-β3 was not required for suppressive activity, as two catalytically inactive mutants, E362G and del, showed a slightly stronger, if any, growth-suppressive activity (Figure 4B), consistent with the assumption that the PLC catalytic activity enhances cellular growth. The PH domain had no effect on cellular growth. The growth-suppressive function of CT was confirmed in vivo: *PLC-β3*$^{-/-}$ KSL cells transduced with CT failed to cause MPD in recipient mice (Figure S8B). KSL cells recovered from such recipient mice showed slower in vitro growth with lower levels of Stat5 phosphorylation than KSL cells from mice that had received empty vector-transduced *PLC-β3*$^{-/-}$ KSL cells (Figures S8C and S8D).

Multimolecular Interactions Involve PLC-β3, Stat5, and SHP-1

We found physical interactions between PLC-β3 and Stat5. Thus, anti-PLC-β3 antibody coimmunoprecipitated Stat5 from Ba/F3 cell lysates (Figure 4D). Low-level coimmunoprecipitation before stimulation was followed by a transient increase with a peak at 1–3 min upon IL-3 stimulation. Reciprocally, PLC-β3 was coimmunoprecipitated with anti-Stat5 antibody (Figure 4D). IL-3-inducible interactions between PLC-β3 and Stat5 were also shown in mouse splenocytes (Figure S9A). Consistent with these biochemical data, confocal imaging analysis showed colocalization of PLC-β3 with phospho-Stat5 in the cytoplasm of IL-3-stimulated Ba/F3 cells (Figure S9B). By contrast, Stat3 was not coimmunoprecipitated with PLC-β3 (data not shown). Given the potential role of SHP-1 in dephosphorylating Stat5 and inhibiting IL-3-dependent cell growth (Paling and Welham, 2002), we examined whether PLC-β3 interacts with SHP-1. Indeed, coimmunoprecipitation was observed between PLC-β3 and SHP-1 in Ba/F3 and spleen cells (Figure 4D and Figure S9A), but not between PLC-β3 and other phosphatases such as SHP-2, PP2A, and PTP-1B, despite their robust expression in Ba/F3 cells (data not shown). PLC-β3/SHP-1 interactions were largely constitutive, but increased by 30%–150% at 10 min stimulation

with IL-3 (Figure 4D). Stat5 also interacted with SHP-1 and this interaction slightly increased at 1 and 10 min stimulation with IL-3 (Figure 4D and Figure S9A). The ability of PLC-β3 CT to interact with SHP-1 and Stat5 were confirmed by in vitro GST fusion protein pull-down assays (Figure S10).

Pairwise interactions among PLC-β3, Stat5, and SHP-1 raised the possibility that these molecules are present in the same multimolecular complex. To test this hypothesis, we performed a series of immunodepletion/immunoprecipitation experiments. Briefly, depletion of one of these three molecules from Ba/F3 lysates abrogated or drastically reduced the interaction between the other two molecules (Figure S11). As these results indicate the presence of a multimolecular complex, we propose to call it the SPS complex, which includes SHP-1, PLC-β3, and Stat5 as components. Pairwise interactions among PLC-β3, SHP-1, and Stat5 were modestly induced upon IL-3 stimulation in nontransduced Ba/F cells and splenocytes from normal mice (Figure 4D and Figure S9A). IL-3-mediated inducibility of interactions among these molecules became more remarkable in Ba/F3 cells overexpressing PLC-β3 (Figure S9C). These results suggest that pairwise interactions among the three proteins, particularly PLC-β3/Stat5 interactions, can be inducible by IL-3 stimulation. As immunodepletion of one component from IL-3-stimulated, PLC-β3-overexpressing Ba/F3 cells completely or near completely abrogated interactions between the other two components (Figure S11), large proportions of these three molecules were interpreted to reside in SPS complexes upon IL-3 stimulation. Furthermore, PLC-β3 deficiency almost abrogated the SHP-1/Stat5 interaction and the motheaten viable (me^v/me^v) mutation in SHP-1 (Tsui et al., 1993) drastically reduced the PLC-β3/Stat5 interaction (Figure 4E). These results suggest that formation of stable SPS complexes require PLC-β3 and normal SHP-1 proteins. By contrast, ~80% reduction in Stat5 expression did not affect the PLC-β3/SHP-1 interaction (Figure 4E), together with our observation of the direct interaction between PLC-β3 and SHP-1 (Figure S10F), suggesting that Stat5 may not be required for the initial assembly of SPS complexes. These results suggest the dynamic nature of the SPS complex, in which PLC-β3 and SHP-1 function as a limiting factor in its assembly.

PLC-β3 Enhances SHP-1-Mediated Dephosphorylation of Stat5

Functional relationship among the components of the SPS complex was assessed in an in vitro phosphatase assay using recombinant SHP-1 and PLC-β3 CT (GST-PLC-β3 CT). The substrate used in this assay was phospho-Stat5 immunoprecipitated from pervanadate-stimulated Daudi cells, which expressed low levels of PLC-β3 (see Figure 7A). Phospho-Stat5 levels were modestly reduced by incubation with WT, but not catalytically inactive D419A, SHP-1 (Figure 4F, lanes 2 and 3), providing the direct evidence that SHP-1 can dephosphorylate phospho-Stat5. More importantly, incubation of phospho-Stat5 with GST-PLC-β3 CT plus WT (but not D419A mutant) SHP-1 drastically reduced phospho-Stat5 levels (Figure 4F, lane 5). Incubation of phospho-Stat5 with GST-PLC-β3 CT alone slightly reduced phosphorylation levels, suggesting that the catalytic activity of the endogenous, Stat5-associated SHP-1 was enhanced with GST-PLC-β3 CT. Indeed, probing the same blot with anti-SHP-1 confirmed the presence of endogenous SHP-1 in Stat5 immunoprecipitates. We next tested the functional relevance of the SPS complex in the cellular context. Coexpression of PLC-β3 and SHP-1 had a stronger inhibitory effect on IL-3-induced Ba/F3 cell proliferation, compared to those of PLC-β3 or SHP-1 alone (Figure 4G). These results suggest that the SPS complex is functional and that PLC-β3 present in the SPS complex augments the phosphatase activity of SHP-1 toward phospho-Stat5.

PLC-β3 CT Cannot Suppress the Proliferative, Myeloid-Differentiative, and MPD-Causing Capabilities of HSC Derived from Motheaten Viable Mice

Given the probable role of the SPS complex in antagonizing Stat5 activation, we investigated whether the apparent MPD in me^v/me^v mice (Figure 5A) has a similar pathogenic mechanism as that in *PLC-β3*$^{-/-}$ mice. Indeed, increased numbers of KSL and GMP cells were present in the BM of me^v/me^v mice (Figure 5B). CD34$^-$ KSL cells from me^v/me^v mice grew faster in vitro with higher levels of Stat5 phosphorylation than WT cells (Figures 5C and 5D) and their in vitro growth was inhibited by DN Stat5 (Figure 5E). The MPD in me^v/me^v mice was BM cell autonomous (Figure S12) and me^v/me^v CD34$^-$ KSL cells transduced with DN Stat5 failed to develop MPD in recipient mice (Figure 5F). Therefore, we concluded that constitutive Stat5 activation is a shared mechanism for MPD development in *PLC-β3*$^{-/-}$ and me^v/me^v mice. Interestingly, in vitro growth of me^v/me^v CD34$^-$ KSL cells was only marginally affected by PLC-β3 CT (Figure 5E) and transduction of me^v/me^v CD34$^-$ KSL cells with full-length PLC-β3 or PLC-β3 CT did not prevent MPD development in recipient mice (Figure 5F), similar to nontransduced (GFP$^-$) cells (Figure 5G). By contrast, me^v/me^v CD34$^-$ KSL cells transduced with WT SHP-1 did not cause MPD in recipient mice. Together with the reduced PLC-β3/Stat5 interaction in me^v/me^v cells (Figure 4E), these results suggest that aberrant SHP-1 proteins encoded by me^v/me^v (Shultz et al., 1993) cannot use the adaptor function of PLC-β3 to suppress Stat5 phosphorylation.

PLC-β3 Haploinsufficiency Cooperates with c-Myc to Transform Fibroblasts and Lymphocytes

To further analyze the transforming ability of PLC-β3-deficient cells, we transfected *PLC-β3*$^{-/-}$ MEFs with V12 H-*ras* or c-*myc*. Unlike active H-*ras*, which induced senescence in WT and *PLC-β3*$^{-/-}$ MEFs (data not shown), c-*myc* induced in vitro transformation in *PLC-β3*$^{+/-}$ and *PLC-β3*$^{-/-}$ MEFs (Figure 6A). In light of this observation, we investigated whether PLC-β3 deficiency can cooperate with c-*myc* to induce in vivo tumor formation, by crossing *PLC-β3*$^{-/-}$ mice with *Eμ-myc* transgenic mice. As reported previously (Adams et al., 1985), *Eμ-myc* transgenic mice developed B cell-lineage lymphomas with a long latency. Lymphoma formation in *Eμ-myc* transgenic mice with heterozygous *PLC-β3*$^{+/-}$ loci was dramatically accelerated (median survival: 100 days in *Eμ-myc;PLC-β3*$^{+/-}$ mice versus >365 in *Eμ-myc;PLC-β3*$^{+/+}$ mice) (Figure 6B). These *Eμ-myc;PLC-β3*$^{+/-}$ lymphomas expressed a pre-B cell phenotype of B220$^+$ IgM$^-$ CD43$^-$ (data not shown). These and *PLC-β3*$^{-/-}$ lymphomas showed higher levels of Stat5 phosphorylation than normal lymphoid tissues (Figure 6C). Importantly, all analyzed *PLC-β3*$^{-/-}$ lymphomas showed as high c-Myc expression as did *Eμ-myc;PLC-β3*$^{+/-}$ lymphomas. On the other hand, the

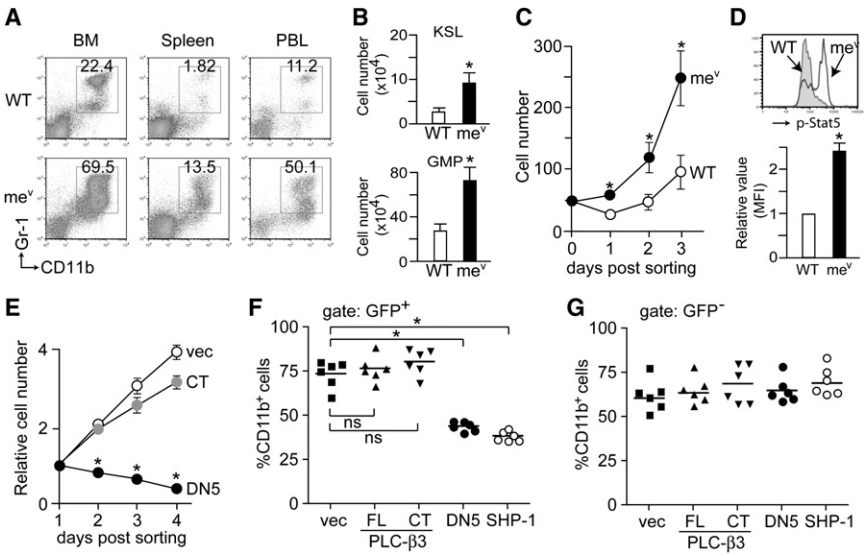

Figure 5. MPD-Causing Ability of HSC-Enriched Cells Derived from Motheaten Viable Mice Depend on Stat5

(A) Flow cytometric analysis of nucleated cells in BM, spleen, and peripheral blood (PBL) of 6- to 8-week-old mice (n = 6). Granulocyte percentages are shown.

(B) Flow cytometric analysis of KSL and GMP in BM (n = 6). *p < 0.05 versus WT cells.

(C) CD34$^-$ KSL cells from 6- to 8-week-old mice (n = 4) were sorted and cultured in IL-3, SCF, IL-11, Flt3L, and TPO. Representative of three independent experiments.

(D) Flow cytometric analysis of phospho-Stat5 levels (n = 4).

(E) *me^v/me^v* CD34$^-$ KSL cells were transduced with a bicistronic retroviral vector expressing DN Stat5, PLC-β3 CT, or empty vector (vec). Growth of GFP$^+$ cells was monitored. *p < 0.05 versus empty vector cells. Results in (B)–(E) represent mean ± SD.

(F and G) *me^v/me^v* CD34$^-$ KSL cells were transduced with the indicated constructs and adoptively transferred to lethally irradiated mice. Two months later, peripheral blood was analyzed by flow cytometry for enumeration of CD11b$^+$ cells in GFP$^+$ donor-derived cells. Similar results were observed 4 months after transfer (data not shown). *p < 0.05; ns, not significant.

expression of PLC-β3 protein in *Eμ-myc;PLC-β3$^{+/-}$* lymphomas was drastically reduced compared to normal lymphoid tissues (Figure 6C). As extensive RT-PCR analyses covering all exon sequences of PLC-β3 mRNA gave the same levels (Figure S13) in WT spleens and two *Eμ-myc;PLC-β3$^{+/-}$* lymphomas (samples 1 and 2 in Figure 6C) and no mutations were found in the PLC-β3 exons (data not shown), the very low expression of PLC-β3 protein in these lymphomas seemed due to abnormal posttranscriptional regulation of PLC-β3 mRNA: stability of the PLC-β3 protein might be low. Alternatively, translation of the PLC-β3 protein might be abnormal and inefficient in *Eμ-myc;PLC-β3$^{+/-}$* lymphomas. Another possibility is somatic-inactivating point mutations in other cases of *Eμ-myc;PLC-β3$^{+/-}$* lymphomas. However, PLC-β3 protein expression in *PLC-β3$^{+/-}$* splenocytes is reduced by about 50% as expected (data not shown), which is consistent with the fact that *PLC-β3$^{+/-}$* mice did not show any abnormal phenotypes. Retroviral expression of DN Stat5 or PLC-β3 CT in *Eμ-myc;PLC-β3$^{+/-}$* lymphoma cells suppressed their in vitro growth and colony formation (Figures 6D and 6E). These results indicate that PLC-β3 haploinsufficiency cooperates with c-Myc to transform fibroblasts and lymphocytes.

Translocations of c-*myc* to immunoglobulin or other gene loci and thus abnormal expression of c-*myc* are causally linked to Burkitt's lymphoma (Boxer and Dang, 2001). Interestingly, two of six Burkitt's lymphoma cell lines tested, i.e., Daudi and Raji, exhibited very low levels (5%–10% that in Ba/F3 cells) of PLC-β3 protein and they had higher basal levels of STAT5 phosphorylation than the other Burkitt's cells with high PLC-β3 expression (Figure 7A). Overexpression of PLC-β3 CT in Daudi and Raji cells blocked their growth (Figure 7B and data not shown) and reduced STAT5 phosphorylation (Figure 7C). Expression of DN STAT5 also blocked the growth of these Burkitt's lymphoma cells (Figure 7D and data not shown), but not that of Ramos cells expressing high levels of PLC-β3 (data not shown). These results together with observations on *PLC-β3$^{-/-}$* and *Eμ-myc;PLC-β3$^{+/-}$* lymphomas are consistent with the notion that reduced or abrogated expression of PLC-β3 may cooperate with active c-Myc to induce lymphoma in mice and humans. In addition to these lymphoid tumor cells, overexpression of full-length PLC-β3 or CT in GM-CSF-dependent TF-1 erythroleukemia cells suppressed GM-CSF-dependent cell growth associated with repressed STAT5 phosphorylation (Figures 7E and 7F); on the other hand, knockdown (to a level of 20%–30% that in Ba/F3 cells) of PLC-β3 expression using lentivirus-mediated RNA interference rendered TF-1 cell growth independent of GM-CSF and associated with increased STAT5 phosphorylation (Figures 7G and 7H). Similarly, overexpression of full-length PLC-β3 or CT suppressed the growth factor-dependent proliferation and/or survival of other human leukemic cell lines such as MEC2 and HL-60 (data not shown). Eleven percent of chronic lymphocytic leukemia (CLL) samples showed low levels of PLC-β3 expression with high phospho-STAT5 levels (Figure 7I and data not shown). The results collectively suggest that reduced expression of PLC-β3 and thus the loss of the SHP-1-mediated Stat5 dephosphorylation mechanism cooperates with active c-*myc* (or an unknown oncogene) to induce lymphoid and myeloid malignancies in mice and humans.

DISCUSSION

This study demonstrates an adaptor function of PLC-β3 that negatively regulates proliferative, survival, and myeloid-differentiative capabilities of HSC-enriched cell populations. PLC-β3 augments SHP-1-mediated deactivation of Stat5 activity (Figure 8). Loss of this regulation seems to lead to MPD development in aged *PLC-β3$^{-/-}$* mice. Long latency suggests that an additional transforming event is required for conversion of *PLC-β3$^{-/-}$* HSC/progenitor cells to malignant cells. Importantly,

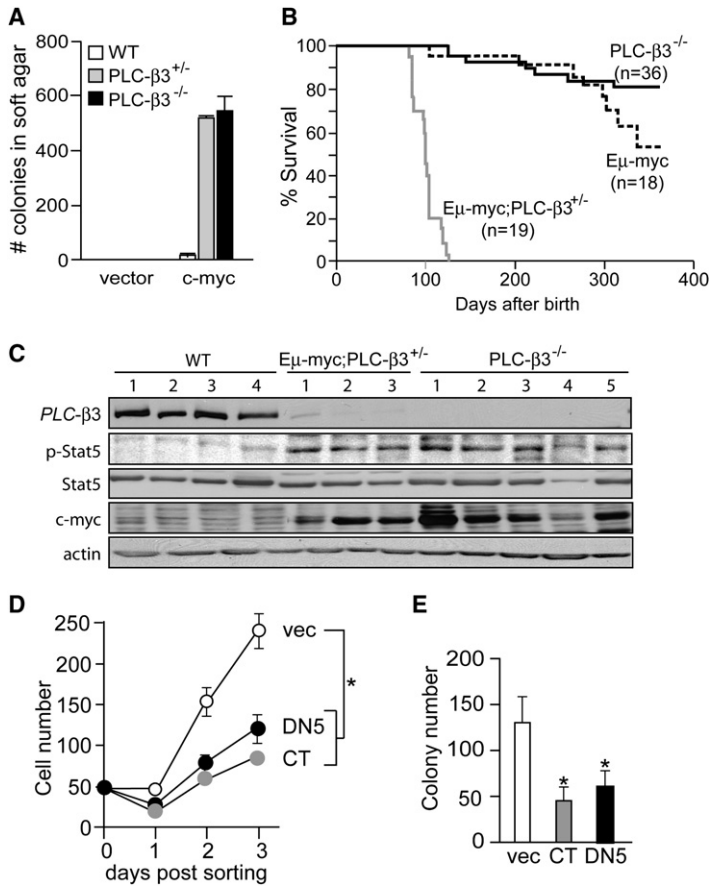

Figure 6. PLC-β3 Deficiency Cooperates with c-Myc to Transform Mouse Fibroblasts and Lymphocytes

(A) MEFs from WT, *PLC-β3*$^{+/-}$, and *PLC-β3*$^{-/-}$ mice (n = 8 each) were transfected with c-*myc* and subjected to semisolid colony-forming assays. Similar results were observed in another experiment.

(B) Survival curves for the indicated mice.

(C) Immunoblot analysis of *PLC-β3*$^{-/-}$ (five independent tumors) and *Eμ-myc;PLC-β3*$^{+/-}$ (three tumors) lymphomas and normal lymphoid tissues. WT samples 1 and 2–4 represent thymus and spleens, respectively, from WT mice.

(D and E) *Eμ-myc;PLC-β3*$^{+/-}$ lymphoma cells were cultured and retrovirally transduced with the indicated genes. Their in vitro growth (D) and colony numbers in semisolid medium (E) were quantified after sorting GFP^{+} cells. Results represent two independent experiments. Results in (A), (D), and (E) represent mean ± SD.

c-*myc* can transform *PLC-β3*$^{+/-}$ MEFs and B cell precursors. Cooperative transformation by active c-*myc* and PLC-β3 deficiency seems to underlie lymphomas in *PLC-β3*$^{-/-}$ and *Eμ-myc; PLC-β3*$^{+/-}$ mice and a subset of human Burkitt's lymphoma. However, c-*myc* expression was not increased in *PLC-β3*$^{-/-}$ KSL cells (data not shown), suggesting that an oncogene other than c-*myc* seems responsible for MPD development.

All the tested MPD, lymphoma, and other tumor cells derived from *PLC-β3*$^{-/-}$ mice had high phospho-Stat5 levels, and DN Stat5 suppressed the growth of *PLC-β3*$^{-/-}$ HSC and lymphoma cells, suggesting that Stat5 activation is part of the necessary transforming processes in these malignancies. Stat5 is frequently activated in leukemia (Benekli et al., 2003; Frohling et al., 2005). Stat5 activation was shown to be essential for MPD or myeloid leukemia induced by the activated oncogenes, such as TEL/JAK2 (Schwaller et al., 2000), TEL/PDGFRB (Cain et al., 2007), and FLT3 ITD (Choudhary et al., 2007), and by deficiencies of SHIP and Lyn/Hck (Xiao et al., 2008). An activating mutation (V617F) in JAK2 was found in human MPDs (Baxter et al., 2005; James et al., 2005; Kralovics et al., 2005; Levine et al., 2005). However, *Jak2* cDNAs cloned from *PLC-β3*$^{-/-}$ KSL cells had the WT sequence around the V617 residue (data not shown). Therefore, it will be interesting to study what kinase activates Stat5 in *PLC-β3*$^{-/-}$ mice.

We provide the direct evidence that SHP-1 can dephosphorylate Stat5 to dampen Stat5 activity. This function is lost in *me*^{v}/*me*^{v} mice; this deficiency underlies the MPD in these mice, as transduction with DN Stat5 inhibited in vitro growth of *me*^{v}/*me*^{v} CD34^{-} KSL cells and MPD development in recipient mice. Transduction of *me*^{v}/*me*^{v} CD34^{-} KSL cells with SHP-1, but not PLC-β3 CT, blocked their MPD-causing capability. These results demonstrate that aberrant SHP-1 proteins generated by the *me*^{v} locus cannot suppress Stat5 phosphorylation. This could be due to the loss of PLC-β3/Stat5 interactions, low enzymatic activity of the mutant SHP-1 proteins, or both.

We have provided biochemical evidence for physical interactions among PLC-β3, Stat5, and SHP-1. Pairwise interactions were modestly enhanced upon IL-3 stimulation, but they were much more strongly induced in Ba/F3 cells overexpressing PLC-β3, suggesting the dynamic nature of complex formation that is under the control of PLC-β3 levels and IL-3 stimulation. However, the structure and function of this complex remained to be defined. Our in vitro phosphatase assays showed that SHP-1 can dephosphorylate phospho-Stat5 on Tyr-694 to deactivate Stat5 and that PLC-β3 CT augments this dephosphorylation reaction. Therefore, we hypothesize that SPS complex formation enhances the activity of SHP-1 to deactivate Stat5 to prevent unchecked Stat5 activation. Further, the dysregulation of this mechanism at the level of HSC may lead to the development of MPD. It is tempting to speculate that similar dysregulation in other hematopoietic or non-hematopoietic cells may also contribute to tumorigenic processes of various malignancies.

PLC-β3 CT can specifically interact with Stat5 and SHP-1. The corresponding CT of turkey PLC-β forms a coiled-coil structure that dimerizes along its long axis, a structure for interactions with GTP-bound Gαq (Singer et al., 2002). This part of PLC-β3 has low sequence similarity (30% identity) to the corresponding region of PLC-β2. Consistent with this and biological differences between *PLC-β3*$^{-/-}$ and *PLC-β2*$^{-/-}$ mice, PLC-β2 did not coimmunoprecipitate with Stat5 or SHP-1 (data not shown). Mutations of Ser-1105 (PKC phosphorylation site) or the C-terminal residues (PDZ domain-binding site) did not affect the growth-suppressive activity. These results indicate that PLC-β3 CT contains a determinant responsible for growth suppression with interaction sites for Stat5 and SHP-1.

Information in the public domain, e.g., the Cancer Genome Anatomy Project website (http://cgap.nci.nih.gov/Chromosomes/), indicates reduced or abrogated expression of PLC-β3 in human

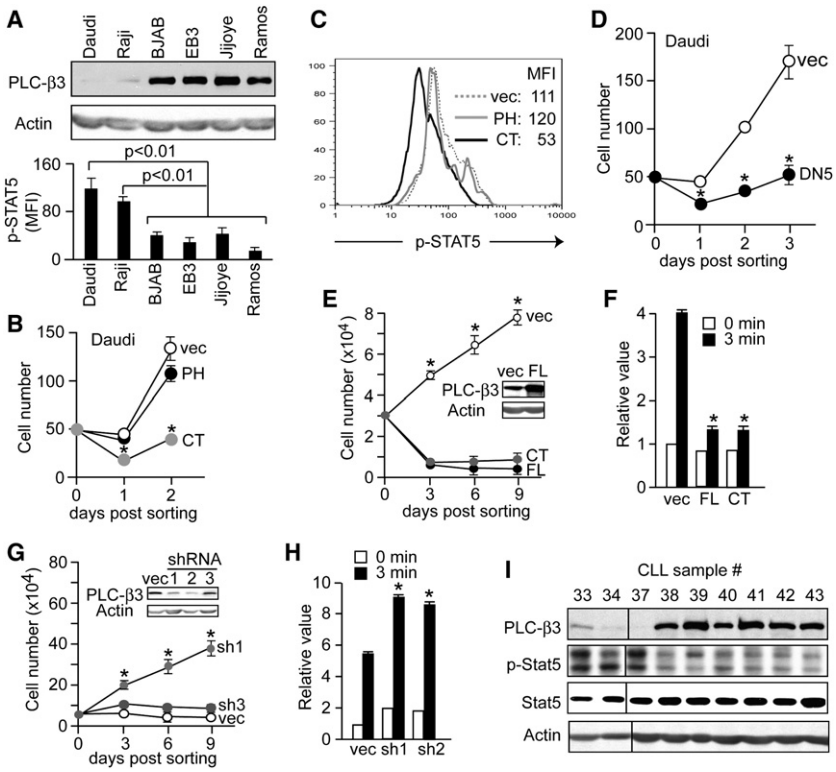

Figure 7. Growth Regulation of Burkitt's Lymphoma and Erythroleukemia Cells by PLC-β3

(A) Daudi and Raji cells, but not other Burkitt's lymphoma cells, express very low levels of PLC-β3 (as shown by immunoblotting) and high levels of phospho-STAT5 (as shown by flow cytometry).

(B–D) Daudi cells were retrovirally transduced with the indicated genes. GFP$^+$ transduced cells were FACS sorted and enumerated (B and D). (C) Phospho-STAT5 levels in the transduced Daudi cells were measured by flow cytometry.

(E and F) TF-1 cells were transduced with full-length (FL) PLC-β3 or CT, and then GFP$^+$ cells were cultured in the presence of GM-CSF. The inset in (E) shows expression of PLC-β3 and (F) shows phospho-STAT5 MFI levels.

(G and H) TF-1 cells were lentivirally transduced with short hairpin RNA (shRNA) constructs targeting the human PLC-β3 gene. The inset shows that sh1 and sh2, but not sh3, constructs efficiently inhibited expression of PLC-β3 protein. (H) Transduced TF-1 cells were stimulated by GM-CSF for 3 min before flow cytometric measurement of phospho-STAT5.

(I) Immunoblot analysis of human CLL. Results in (A), (B), and (D)–(H) represent mean ± SD.

malignancies. A recent genome-wide analysis of genetic alterations in acute lymphocytic leukemia (ALL) demonstrated that a small number of ALL patients have deletions of the region of chromosome 11 including the *PLC-β3* gene (Mullighan et al., 2007). Furthermore, the Oncomine database (Rhodes et al., 2004) shows that reduced expression of *PLC-β3* mRNA is associated with higher grades of bladder carcinoma ($p = 4.2 \times 10^{-7}$). We also found loss or reduced PLC-β3 expression in human tumor cell lines (Figure 7I and data not shown). Therefore, reduced or abrogated expression of PLC-β3 may play a role in the tumorigenic process of human malignancies.

Regulation of PLC-β3 expression has not been well studied. Therefore, it is not clear how PLC-β3 expression is reduced or abrogated in tumors. One obvious possibility is deletions of the chromosomal region encompassing the *PLC-β3* gene, as shown in the aforementioned ALL cases. Another possible mechanism is DNA methylation of the gene promoter. Indeed, treatment with decitabine, an inhibitor of the DNA methyltransferase activity, restored PLC-β3 expression in Daudi cells (data not shown). There might be other unknown mechanisms for reduced expression. However, simple mutations or gene fusions do not seem to be involved in reduced or abrogated expression of PLC-β3, as such mutations in the human *PLC-β3* gene were not found in 136 tumor samples (COSMIC website, http://www.sanger.ac.uk/genetics/CGP/cosmic/). However, this issue warrants further investigation.

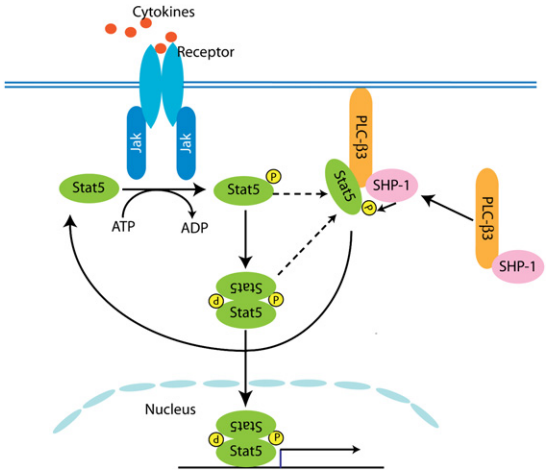

Figure 8. Proposed Mechanism for PLC-β3-Mediated Inhibition of Stat5 Overactivation

Following cytokine stimulation, the Jak-Stat pathway is activated, leading to activation of Stat target genes. PLC-β3/ SHP-1 complexes recruit phosphorylated Stat5 to its C-terminal domain to form SPS complexes. PLC-β3 in the complexes augments the capability of SHP-1 of dephosphorylating Stat5 and inhibiting its nuclear translocation. At this point we do not know whether monomeric or dimeric phosphorylated Stat5 is recruited.

EXPERIMENTAL PROCEDURES

Mice and MPD

PLC-β3$^{-/-}$ and *PLC-β2*$^{-/-}$ mice were described previously (Li et al., 2000). *Me*^{v}, C57BL/6-Ly5.1, and the *Rag2*$^{-/-}$-Ly5.1 mice were purchased from the Jackson Laboratory and Taconic, respectively. *Stat5 floxed* mice (Cui et al., 2004) with *Mx1-cre* will be described elsewhere (A.K. and L.H., unpublished data). For the definition of MPD, we followed the criteria adopted by the Mouse Models of Human Cancers Consortium (Kogan et al., 2002) and by Passegue et al. (2004). The Animal Care and Use Committee of the La Jolla Institute for Allergy and Immunology approved all mouse experiments.

Identification, Purification, and Proliferation of HSC

See the Supplemental Data for the identification and purification of HSC. For proliferation assays, KSL or $CD34^-$ KSL cells were sorted into a 96 well round bottom plate (one cell per well) in 200 μl of IMDM containing 5% FBS, 50 μM 2-mercaptoethanol, and either IL-3 (10 ng/ml) alone or a cocktail of stem cell factor (SCF), IL-3, Flt3L, thrombopoietin (TPO), and IL-11, and incubated at 37°C for the indicated periods. The number of cells per well were visually determined under an inverted microscope. In some experiments, 50 or 150 $CD34^-$ KSL cells were sorted per well and a cocktail of SCF, Flt3L, and IL-11 was added. For BrdU incorporation, cell cycle analysis, and analysis of phosphorylated signaling molecules in HSC, see the Supplemental Data.

Retroviral Transduction

Recombinant retroviruses were produced as previously described (Kato et al., 2005). Sorted $CD34^-$ KSL cells (150 cells/well) were incubated in α-MEM supplemented with 1% FBS, SCF, and human TPO for 24 hr, and then transduced with a retrovirus vector (pMX-GFP-DN Stat5 or DN Stat3; pMIG-SHP-1 or pMIG-PLC-β3 or -CT) in the presence of protamine sulfate (10 μg/ml) and recombinant fibronectin fragment (1 μg/ml) for 24 hr. Transduced cells were further subjected to liquid (in the presence of SCF, Flt-3L, and IL-11) or semi-solid cultures (MethoCult M3434 from StemCell Technologies). In these experiments, transduction efficiency was ~80% as judged by GFP expression by epifluorescence microscopy.

Transplantation of Hematopoietic Cells

BM cells (2×10^6 cells in 400 μl PBS) were injected into the tail vein of lethally (960 rad) irradiated recipient mice (C57BL/6-Ly5.1; 8–10 weeks old). For transplantation of HSC and progenitors, FACS-sorted $CD34^-$ KSL, $CD34^+$ KSL, CMP, and GMP were injected into sublethally irradiated (450 rad) *Rag2*$^{-/-}$-Ly5.1 recipient mice. We also transplanted retrovirally transduced HSCs into lethally irradiated C57BL/6-Ly5.1 mice together with 2.5×10^5 Sca-1-depleted C57BL/6-Ly5.1 helper BM cells.

Transduction, Coimmunoprecipitation, and Immunodepletion of Ba/F3 Cells

Ba/F3 cells were cultured in IL-3-containing medium and transduced with a retrovirus vector (pMIG-myc-PLC-β3 WT or mutants). Forty-eight hours later, transduced GFP^+ cells were FACS-sorted into a 96 well plate at a density of 50 cells per well and cultured in the presence of IL-3. For coimmunoprecipitation, transduced cells deprived of IL-3 were stimulated with 10 ng/ml of IL-3, and cell lysates were immunoprecipitated with anti-Stat5 (C-17), anti-PLC-β3 (C-20) (or anti-myc), or anti-SHP-1 (C-19) antibodies (all from Santa Cruz Biotechnology). For immunodepletion, cell lysates were precipitated with anti-Stat5, anti-PLC-β3, or anti-SHP-1 antibodies, and supernatants were collected for coimmunoprecipitation.

In Vitro Phosphatase Assay

In vitro phosphatase assay was performed essentially as described (Nakahira et al., 2007). In brief, phospho-Stat5 was immunoprecipitated from pervanadate-treated Daudi cells and incubated with GST-tagged proteins in 25 mM HEPES (pH 7.5), 5 mM EDTA, and 10 mM DTT at 30°C for 1 hr. GST-SHP-1 WT or D419A mutant was phosphorylated by Lyn precipitated from Ba/F3 cells in vitro.

Human Samples

Peripheral blood samples were collected from patients with human hematopoietic malignancies. Leukocytes were lysed in SDS sample buffer and analyzed by western blotting. The study protocols were approved by the Human Subjects Research Ethics Board of the University of Western Ontario. Informed consent was obtained from each study subject.

SUPPLEMENTAL DATA

Supplemental Data include Supplemental Experimental Procedures, 13 figures, and six tables and can be found with this article online at http://www.cell.com/cancer-cell/supplemental/S1535-6108(09)00182-2.

ACKNOWLEDGMENTS

We thank Federico Caligaris-Cappio, James N. Ihle, Toshio Kitamura, John Ryan, Reuben P. Siraganian, Jean Y.J. Wang, and Kirin Pharma for kindly providing reagents; and Shuji Ueda for making some constructs. We are grateful to Michael Poderycki and Yu Kawakami for critical reading of the manuscript. This study was supported in part by grants from the National Institutes of Health to T.K. W.X. was supported in part by funds from the Diabetes and Immune Disease National Research Institute. This is Publication 769 from the La Jolla Institute for Allergy and Immunology. W.X., H.H., Y. Kato, and H.Y. performed experiments; D.W., A.K., and L.H. provided critical reagents; H.K., L.F.B., R.S.D., L.A.C., J.M., C.C.H., A.X., and T.J.K. provided human samples; W.X., Y. Kawakami, A.I., H.N., and T.K. designed experiments and analyzed results; W.X. and T.K. wrote the manuscript. The authors declare that they have no competing financial interests.

Received: December 24, 2008
Revised: March 20, 2009
Accepted: May 28, 2009
Published: August 3, 2009

REFERENCES

Adams, J.M., Harris, A.W., Pinkert, C.A., Corcoran, L.M., Alexander, W.S., Cory, S., Palmiter, R.D., and Brinster, R.L. (1985). The c-myc oncogene driven by immunoglobulin enhancers induces lymphoid malignancy in transgenic mice. Nature *318*, 533–538.

Alexander, W.S., and Hilton, D.J. (2004). The role of suppressors of cytokine signaling (SOCS) proteins in regulation of the immune response. Annu. Rev. Immunol. *22*, 503–529.

Bach, T.L., Chen, Q.M., Kerr, W.T., Wang, Y., Lian, L., Choi, J.K., Wu, D., Kazanietz, M.G., Koretzky, G.A., Zigmond, S., et al. (2007). Phospholipase cbeta is critical for T cell chemotaxis. J. Immunol. *179*, 2223–2227.

Baxter, E.J., Scott, L.M., Campbell, P.J., East, C., Fourouclas, N., Swanton, S., Vassiliou, G.S., Bench, A.J., Boyd, E.M., Curtin, N., et al. (2005). Acquired mutation of the tyrosine kinase JAK2 in human myeloproliferative disorders. Lancet *365*, 1054–1061.

Benekli, M., Baer, M.R., Baumann, H., and Wetzler, M. (2003). Signal transducer and activator of transcription proteins in leukemias. Blood *101*, 2940–2954.

Boxer, L.M., and Dang, C.V. (2001). Translocations involving c-myc and c-myc function. Oncogene *20*, 5595–5610.

Bunting, K.D., Bradley, H.L., Hawley, T.S., Moriggl, R., Sorrentino, B.P., and Ihle, J.N. (2002). Reduced lymphomyeloid repopulating activity from adult bone marrow and fetal liver of mice lacking expression of STAT5. Blood *99*, 479–487.

Cain, J.A., Xiang, Z., O'Neal, J., Kreisel, F., Colson, A., Luo, H., Hennighausen, L., and Tomasson, M.H. (2007). Myeloproliferative disease induced by TEL-PDGFRB displays dynamic range sensitivity to Stat5 gene dosage. Blood *109*, 3906–3914.

Camps, M., Carozzi, A., Schnabel, P., Scheer, A., Parker, P.J., and Gierschik, P. (1992). Isozyme-selective stimulation of phospholipase C-beta 2 by G protein beta gamma-subunits. Nature *360*, 684–686.

Choudhary, C., Brandts, C., Schwable, J., Tickenbrock, L., Sargin, B., Ueker, A., Bohmer, F.D., Berdel, W.E., Muller-Tidow, C., and Serve, H. (2007). Activation mechanisms of STAT5 by oncogenic Flt3-ITD. Blood *110*, 370–374.

Cui, Y., Riedlinger, G., Miyoshi, K., Tang, W., Li, C., Deng, C.X., Robinson, G.W., and Hennighausen, L. (2004). Inactivation of Stat5 in mouse mammary epithelium during pregnancy reveals distinct functions in cell proliferation, survival, and differentiation. Mol. Cell. Biol. *24*, 8037–8047.

Emanuel, P.D., Bates, L.J., Castleberry, R.P., Gualtieri, R.J., and Zuckerman, K.S. (1991). Selective hypersensitivity to granulocyte-macrophage colony-stimulating factor by juvenile chronic myeloid leukemia hematopoietic progenitors. Blood *77*, 925–929.

Frohling, S., Scholl, C., Gilliland, D.G., and Levine, R.L. (2005). Genetics of myeloid malignancies: pathogenetic and clinical implications. J. Clin. Oncol. *23*, 6285–6295.

Ilaria, R.L., Jr., Hawley, R.G., and Van Etten, R.A. (1999). Dominant negative mutants implicate STAT5 in myeloid cell proliferation and neutrophil differentiation. Blood *93*, 4154–4166.

James, C., Ugo, V., Le Couedic, J.P., Staerk, J., Delhommeau, F., Lacout, C., Garcon, L., Raslova, H., Berger, R., Bennaceur-Griscelli, A., et al. (2005). A unique clonal JAK2 mutation leading to constitutive signalling causes polycythaemia vera. Nature *434*, 1144–1148.

Jiao, H., Berrada, K., Yang, W., Tabrizi, M., Platanias, L.C., and Yi, T. (1996). Direct association with and dephosphorylation of Jak2 kinase by the SH2-domain-containing protein tyrosine phosphatase SHP-1. Mol. Cell. Biol. *16*, 6985–6992.

Kato, Y., Iwama, A., Tadokoro, Y., Shimoda, K., Minoguchi, M., Akira, S., Tanaka, M., Miyajima, A., Kitamura, T., and Nakauchi, H. (2005). Selective activation of STAT5 unveils its role in stem cell self-renewal in normal and leukemic hematopoiesis. J. Exp. Med. *202*, 169–179.

Katz, A., Wu, D., and Simon, M.I. (1992). Subunits beta gamma of heterotrimeric G protein activate beta 2 isoform of phospholipase C. Nature *360*, 686–689.

Klingmuller, U., Lorenz, U., Cantley, L.C., Neel, B.G., and Lodish, H.F. (1995). Specific recruitment of SH-PTP1 to the erythropoietin receptor causes inactivation of JAK2 and termination of proliferative signals. Cell *80*, 729–738.

Kogan, S.C., Ward, J.M., Anver, M.R., Berman, J.J., Brayton, C., Cardiff, R.D., Carter, J.S., de Coronado, S., Downing, J.R., Fredrickson, T.N., et al. (2002). Bethesda proposals for classification of nonlymphoid hematopoietic neoplasms in mice. Blood *100*, 238–245.

Kondo, M., Wagers, A.J., Manz, M.G., Prohaska, S.S., Scherer, D.C., Beilhack, G.F., Shizuru, J.A., and Weissman, I.L. (2003). Biology of hematopoietic stem cells and progenitors: implications for clinical application. Annu. Rev. Immunol. *21*, 759–806.

Kralovics, R., Passamonti, F., Buser, A.S., Teo, S.S., Tiedt, R., Passweg, J.R., Tichelli, A., Cazzola, M., and Skoda, R.C. (2005). A gain-of-function mutation of JAK2 in myeloproliferative disorders. N. Engl. J. Med. *352*, 1779–1790.

Kyba, M., Perlingeiro, R.C., Hoover, R.R., Lu, C.W., Pierce, J., and Daley, G.Q. (2003). Enhanced hematopoietic differentiation of embryonic stem cells conditionally expressing Stat5. Proc. Natl. Acad. Sci. USA *100* (*Suppl 1*), 11904–11910.

Lee, S.B., Shin, S.H., Hepler, J.R., Gilman, A.G., and Rhee, S.G. (1993). Activation of phospholipase C-beta 2 mutants by G protein alpha q and beta gamma subunits. J. Biol. Chem. *268*, 25952–25957.

Levine, R.L., Wadleigh, M., Cools, J., Ebert, B.L., Wernig, G., Huntly, B.J., Boggon, T.J., Wlodarska, I., Clark, J.J., Moore, S., et al. (2005). Activating mutation in the tyrosine kinase JAK2 in polycythemia vera, essential thrombocythemia, and myeloid metaplasia with myelofibrosis. Cancer Cell *7*, 387–397.

Levy, D.E., and Darnell, J.E., Jr. (2002). Stats: transcriptional control and biological impact. Nat. Rev. Mol. Cell Biol. *3*, 651–662.

Li, Z., Jiang, H., Xie, W., Zhang, Z., Smrcka, A.V., and Wu, D. (2000). Roles of PLC-beta2 and -beta3 and PI3Kgamma in chemoattractant-mediated signal transduction. Science *287*, 1046–1049.

Lilly, M., and Kraft, A. (1997). Enforced expression of the Mr 33,000 Pim-1 kinase enhances factor-independent survival and inhibits apoptosis in murine myeloid cells. Cancer Res. *57*, 5348–5355.

Matsumoto, A., Masuhara, M., Mitsui, K., Yokouchi, M., Ohtsubo, M., Misawa, H., Miyajima, A., and Yoshimura, A. (1997). CIS, a cytokine inducible SH2 protein, is a target of the JAK-STAT5 pathway and modulates STAT5 activation. Blood *89*, 3148–3154.

Mui, A.L., Wakao, H., O'Farrell, A.M., Harada, N., and Miyajima, A. (1995). Interleukin-3, granulocyte-macrophage colony stimulating factor and interleukin-5 transduce signals through two STAT5 homologs. EMBO J. *14*, 1166–1175.

Mullighan, C.G., Goorha, S., Radtke, I., Miller, C.B., Coustan-Smith, E., Dalton, J.D., Girtman, K., Mathew, S., Ma, J., Pounds, S.B., et al. (2007). Genome-wide analysis of genetic alterations in acute lymphoblastic leukaemia. Nature *446*, 758–764.

Nakahira, M., Tanaka, T., Robson, B.E., Mizgerd, J.P., and Grusby, M.J. (2007). Regulation of signal transducer and activator of transcription signaling by the tyrosine phosphatase PTP-BL. Immunity *26*, 163–176.

Nosaka, T., Kawashima, T., Misawa, K., Ikuta, K., Mui, A.L., and Kitamura, T. (1999). STAT5 as a molecular regulator of proliferation, differentiation and apoptosis in hematopoietic cells. EMBO J. *18*, 4754–4765.

O'Shea, J.J., Gadina, M., and Schreiber, R.D. (2002). Cytokine signaling in 2002: new surprises in the Jak/Stat pathway. Cell *109* (*Suppl*), S121–S131.

Paling, N.R., and Welham, M.J. (2002). Role of the protein tyrosine phosphatase SHP-1 (Src homology phosphatase-1) in the regulation of interleukin-3-induced survival, proliferation and signalling. Biochem. J. *368*, 885–894.

Passegue, E., Wagner, E.F., and Weissman, I.L. (2004). JunB deficiency leads to a myeloproliferative disorder arising from hematopoietic stem cells. Cell *119*, 431–443.

Reya, T., Morrison, S.J., Clarke, M.F., and Weissman, I.L. (2001). Stem cells, cancer, and cancer stem cells. Nature *414*, 105–111.

Rhee, S.G. (2001). Regulation of phosphoinositide-specific phospholipase C. Annu. Rev. Biochem. *70*, 281–312.

Rhodes, D.R., Yu, J., Shanker, K., Deshpande, N., Varambally, R., Ghosh, D., Barrette, T., Pandey, A., and Chinnaiyan, A.M. (2004). ONCOMINE: a cancer microarray database and integrated data-mining platform. Neoplasia *6*, 1–6.

Sawyers, C.L. (1999). Chronic myeloid leukemia. N. Engl. J. Med. *340*, 1330–1340.

Sawyers, C.L., McLaughlin, J., and Witte, O.N. (1995). Genetic requirement for Ras in the transformation of fibroblasts and hematopoietic cells by the Bcr-Abl oncogene. J. Exp. Med. *181*, 307–313.

Schindler, C., Levy, D.E., and Decker, T. (2007). JAK-STAT signaling: from interferons to cytokines. J. Biol. Chem. *282*, 20059–20063.

Schuringa, J.J., Chung, K.Y., Morrone, G., and Moore, M.A. (2004). Constitutive activation of STAT5A promotes human hematopoietic stem cell self-renewal and erythroid differentiation. J. Exp. Med. *200*, 623–635.

Schwaller, J., Parganas, E., Wang, D., Cain, D., Aster, J.C., Williams, I.R., Lee, C.K., Gerthner, R., Kitamura, T., Frantsve, J., et al. (2000). Stat5 is essential for the myelo- and lymphoproliferative disease induced by TEL/JAK2. Mol. Cell *6*, 693–704.

Shuai, K. (2000). Modulation of STAT signaling by STAT-interacting proteins. Oncogene *19*, 2638–2644.

Shultz, L.D., Schweitzer, P.A., Rajan, T.V., Yi, T., Ihle, J.N., Matthews, R.J., Thomas, M.L., and Beier, D.R. (1993). Mutations at the murine motheaten locus are within the hematopoietic cell protein-tyrosine phosphatase (Hcph) gene. Cell *73*, 1445–1454.

Singer, A.U., Waldo, G.L., Harden, T.K., and Sondek, J. (2002). A unique fold of phospholipase C-beta mediates dimerization and interaction with G alpha q. Nat. Struct. Biol. *9*, 32–36.

Skorski, T., Bellacosa, A., Nieborowska-Skorska, M., Majewski, M., Martinez, R., Choi, J.K., Trotta, R., Wlodarski, P., Perrotti, D., Chan, T.O., et al. (1997). Transformation of hematopoietic cells by BCR/ABL requires activation of a PI-3k/Akt-dependent pathway. EMBO J. *16*, 6151–6161.

Snow, J.W., Abraham, N., Ma, M.C., Abbey, N.W., Herndier, B., and Goldsmith, M.A. (2002). STAT5 promotes multilineage hematolymphoid development in vivo through effects on early hematopoietic progenitor cells. Blood *99*, 95–101.

Tanaka, T., Soriano, M.A., and Grusby, M.J. (2005). SLIM is a nuclear ubiquitin E3 ligase that negatively regulates STAT signaling. Immunity *22*, 729–736.

Tsui, H.W., Siminovitch, K.A., de Souza, L., and Tsui, F.W. (1993). Motheaten and viable motheaten mice have mutations in the haematopoietic cell phosphatase gene. Nat. Genet. *4*, 124–129.

Warmuth, M., Kim, S., Gu, X.J., Xia, G., and Adrian, F. (2007). Ba/F3 cells and their use in kinase drug discovery. Curr. Opin. Oncol. *19*, 55–60.

Xiao, W., Hong, H., Kawakami, Y., Lowell, C.A., and Kawakami, T. (2008). Regulation of myeloproliferation and M2 macrophage programming in mice by Lyn/Hck, SHIP, and Stat5. J. Clin. Invest. *118*, 924–934.

Yoshimura, A., Ichihara, M., Kinjyo, I., Moriyama, M., Copeland, N.G., Gilbert, D.J., Jenkins, N.A., Hara, T., and Miyajima, A. (1996). Mouse oncostatin M: an immediate early gene induced by multiple cytokines through the JAK-STAT5 pathway. EMBO J. *15*, 1055–1063.